Article

Not peer-reviewed version

Synergistic Zinc(II) and Formate Doping of alpha-$FAPbI_3$ Perovskite: Thermal Stabilization and Enhanced Photoluminescence Lifetime

Merk M. Hoeksma and René M. Williams *

Posted Date: 13 November 2023

doi: 10.20944/preprints202311.0730.v1

Keywords: solar cells; formamidinium; lead; iodide; alloys

Article

Synergistic Zinc(II) and Formate Doping of α-$FAPbI_3$ Perovskite: Thermal Stabilization and Enhanced Photoluminescence Lifetime

Merk M. Hoeksma and René M. Williams *

Molecular Photonics Group, van 't Hoff Institute for Molecular Sciences (HIMS), Universiteit van Amsterdam, Science Park 904, 1098 XH Amsterdam, Netherlands

* Correspondence: r.m.williams@uva.nl

Abstract: Adding zinc (II) and formate anions improves the thermal phase-stability of α-$FAPbI_3$ materials and the spin-coated thin films of such doped $FAPbI_3$ show an increased emission lifetime of up to 3.7 µs on quartz. This work investigates the effects of zinc and formate on the stability and time-resolved photoluminescence of $FAPbI_3$ perovskites for solar cell applications. Perovskite samples with varying concentrations of zinc and formate were made by incorporating different amounts of zinc formate and zinc iodide and characterized with XRD. Doping levels of 1.7% Zn(II) and 1.0% formate (relative to Pb) seem optimal. The thermal stability of the perovskite powders and thin films were assessed. XRD was virtually unchanged after 6 months. The time-resolved photoluminescence spectroscopy of the doped spin-coated perovskite samples is reported. The results show that synergy between an anionic and a cationic dopant can take place, making the perovskite thermally more stable with a longer charge carrier lifetime.

Keywords: solar cells; formamidinium; lead; iodide; alloys

1. Introduction

Combatting the climate change that started since the industrial revolution, is one of today's most significant challenges [1].To succeed in this challenge, greenhouse gas emissions must be drastically reduced and electrification of society and industry is the target. In 2021 about a quarter of the global energy was generated in a renewable way, and only 13% by solar energy [2]. Improving the cost and availability of solar panels can significantly increase the global amount of electricity obtained from solar energy.

The past two decades have seen a significant increase in research into new materials for solar cells and one of the most promising candidates are the metal halide perovskites. Since the first report describing the use of these perovskites as light-absorbing material in solar cells in 2009, the power conversion efficiency of the perovskite solar cells has been improved from 3.8% [3] to over 26% in 2023 [4]. Two factors that have significantly contributed to the rise of perovskites in solar cell research are the cheap materials and the relative ease at which devices can be produced. With the focus on performance over the past decade, the challenge now lies in understanding and improving the stability and longevity of perovskite solar cells. A similar operating lifetime as for silicon solar cells should be achieved for market adaptation.

In our previous work with Muscarella et al., the effect of Zn(II) on the stability [5] and performance [6] of perovskite materials was investigated. It was found that incorporating Zn(II) into the perovskite structure results in improved stability and an increased power conversion efficiency. Zinc is a good dopant for B-site substitution, with 2.5% seeming close to the optimum.

It should be noted that interface engineering has been recently reported with Zn(II) materials, giving 23.25% PCE [7]. Regarding X-site doping formate anions are an excellent option. One of the highest recently published performances was by Jeong et al. [8], who used formate (2%) as an additive and produced a cell with a certified efficiency of 25.2%.

 doi:10.20944/preprints202311.0730.v1

The primary objective of the study presented here is to explore the influence of simultaneous doping with zinc(II) and formate anions on the stability and performance of $FAPbI_3$ perovskites. We combine B and X-site doping in formamidium lead triiodide. Experiments were conducted involving the fabrication of perovskite samples with varying concentrations of zinc and formate. These samples were fabricated by incorporating different amounts of zinc formate and zinc iodide into the precursor solutions and making powdered perovskites and thin films, the latter characterized with XRD. The performance of the perovskite thin films was evaluated using time-resolved photoluminescence (TR-PL) spectroscopy. TR-PL spectroscopy enables the characterization of the decay dynamics of excited states in materials. By measuring the decay time of the excited states in the perovskite samples, information is gathered about the potential performance of the perovskite in solar cells, focused on radiative charge recombination.

2. Experimental:

2.1. $FAPbI_3$ synthesis

The synthesis of $FAPbI_3$ was performed using the method published by Tong et al. [9]. Formamidinium acetate (1.05 g) was dissolved in 1.5 mL of HI in H_2O solution (57 wt.%). While stirring, PbI_2 (4.61 g) was added to the solution. Not everything dissolved, and then 5 mL of GBL was added. When everything had dissolved, the solution was heated at 95°C for 1 hour. The yellow-orange crystals were filtered using a frit filter and reduced pressure and then transferred to a round-bottom flask, and heated at 150°C for 2 hours. The black spikey crystals were then washed thoroughly using diethyl ether, and the diethyl ether was removed using vacuum filtration. The washing was done by transferring the crystals to the frit filter and then submerging them in diethyl ether. Using a spatula the larger crystals were broken up. The crystals were transferred to another round-bottom flask and heated for another three hours at 150°C. Black crystals were collected. In general, these black α-$FAPbI_3$ crystals will turn yellow within 24 hours, even in the dark. If not properly washed with diethyl ether, traces of acetate can remain in the $FAPbI_3$ product.

It can be noted that lead acetate is used in methyl ammonium-based perovskites as an additive to slow down the crystallization in thin films, for example, leading to larger grains and fewer pinholes in the crystal structure [10]. More recently, lead acetate was used as a starting material for making perovskite layers with a mix of formamidinium and cesium. In this example, the crystallization is also controlled by the acetate, by evaporating the acetate as ammonium acetate (the ammonium is added as a salt with the X anion) [11].

2.2. Precursor solution preparation for spin coating

A general procedure for the preparation of precursor solutions for spin coating is as follows. An amount of $FAPbI_3$ was added to a sample flask. According to this amount, the amount of $ZnFo_2$ and ZnI_2 that should be added for the desired doping percentages are calculated and subsequently added, as well as other additives. The additives are calculated in molar percentages compared to the amount of lead in the base $FAPbI_3$. Subsequently, solvent is added, and the solution is mixed with a small magnetic stirring rod until dissolved. To make sure all solids have dissolved, the solution is also sonicated.

The typical compositions (see Table 1) and procedures for the precursor solutions used in the experiments are given below. Note that the MACl is added to aid the formation of thin films. Without MACl we were unable to produce films of good quality. In literature, MACl is also often added in quantities up to 35 mol% [8]. An alternative that was also tested is MABr, but this induces Br incorporation.

 doi:10.20944/preprints202311.0730.v1

Table 1. The contents of the precursor solutions for the preparation of the spin-coated perovskite films with increasing concentrations of zinc formate. On the left side of the table are the amounts that were added to the precursor solution. On the right side of the table the calculated mol% compared to the amount of Pb is displayed as well as the sum of Zn and Fo doping.

Sample Code	$FAPbI_3$ (mg)	$ZnFo_2$ (mg)	ZnI_2 (mg)	MACl mg (mol%)	% Zn	% Fo	% total
1	800.2	0.9	5.2	18.5 (21.7)	1.7	1.0	2.7
2	806.5	2.0	6.9	21.2 (24.6)	2.6	2.0	4.6
3	806.1	3.0	9.3	19.9 (23.1)	3.8	3.0	6.8

2.3. Perovskite powders

The precursor solutions for the preparation of the perovskite powders were made by dissolving the amounts of $ZnFo_2$ and $FAPbI_3$ that can be seen in Table 2 in 0.15 mL of DMSO. To fully dissolve the solids, the mixture was sonicated for up to 40 minutes at 35°C. The goal was to get the highest concentration possible.

Table 2. The contents of the precursor solutions for the preparation of the perovskite powders with increasing concentrations of zinc formate.

Sample Code	$FAPbI_3$ (mg)	$ZnFo_2$ (mg)	% Zn	% Fo	% total
0.0%	295.6	0.0	0.00	0.00	0.00
0.5%	299.0	0.3	0.41	0.82	1.23
1.0%	297.8	0.7	0.96	1.92	2.88
2.0%	297.3	1.7	2.33	4.66	6.99
3.0%	297.0	2.2	3.02	6.04	9.06
4.0%	298.2	2.9	3.96	7.92	11.88

2.4. Thin films for XRD and TR-PL

Three different precursor solutions were made for the spin-coating, with a low, medium and high amount of doping. The different precursor solutions were made by dissolving the specified amounts of $FAPbI_3$, $ZnFo_2$, ZnI_2, and MACl in 1.1 mL of a 1:4 mixture of DMSO:DMF.

The solutions were stirred using a small magnetic stirring rod for 25 minutes and also sonicated for 25 minutes until everything had dissolved. To make sure no particulates would be present in the spin coating process the solutions were filtered using PTFE-syringe filters.

Similar to what has been reported in literature, precursor solutions that have aged (e.g. for 30 days) produce layers of lower quality.[12]

2.5. Doped powder preparation

The preparation of the precursor solutions for the doped perovskite powders can be found in the previous section. The solutions were drop-cast into Petri dishes in tiny drops using a syringe and needle. The Petri dishes were heated at 180°C directly on a hotplate. The small drops turned black, and some vapor escaped, using a spatula the drops were then scraped off and made into a powder. 20-25 minutes was the minimum time for the drops to dry enough to scrape them off. Using smaller drops helps in drying properly.

2.6. Substrate cleaning

All substrates were cleaned by sonicating in a beaker with milli-Q water with Helmanex III soap for 15 minutes. The substrates were then rinsed with milli-Q water and placed back in a rinsed Teflon sample holder. After this, the samples are sonicated for 15 minutes in acetone and subsequently 2-propanol, also for 15 minutes. After sonication, the substrates were dried with compressed air and lastly treated with ozone in a UV-ozone oven for at least a half hour.

 doi:10.20944/preprints202311.0730.v1

For all of the cleaning steps, it is best if the slides are placed in the sample holder in a way that there is the least amount of contact possible between the sample holder and the substrates. This is done because, sometimes, especially when using thicker substrates, the substrates sit tight in the slots and will not get cleaned properly. This can later show up during spin coating, leading to uncoated edges on the substrates. To ensure the sample holders do not affect the cleaning in the UV-ozone oven, the substrates can be laid on a clean glass plate in the UV-ozone oven with the side where the perovskite will be deposited facing up. Quartz substrates were obtained from Osilla. Glass plates from Menzel were also used.

2.7. Spin coating

The thin film samples were produced by spin coating. The techniques and parameters used during spin coating were varied and experimented with. A very useful resource used was the Osilla Spin coating guide [13]. The procedure that was ultimately found to produce good quality films reliably is as follows. For spin coating the substrates are taken out of the UV-ozone oven one by one and the oven is switched on again for the remaining substrates. The substrate is centered on the table by eye and the suction is switched on. Then, on the spin coater, a gentle stream of N2 is blown over the substrate for about three seconds to remove any possible dust particles. At 3000 rpm, with no ramp, the sample was spun for 30 seconds, then after 3-4 seconds of spinning, 0.06 mL of precursor solution was put on the center of the spinning substrate as close as possible but without touching the surface, this can be done using a micropipette or a syringe and needle, but when using a needle extra care has to be taken that the solution is not applied too fast. The micropipette was found to create less dripping. After spinning for 30 seconds, the sample is spun for another 30 seconds at 2500 rpm. After a few seconds, 0.7-0.8 mL of diethyl ether (DEE) is applied to the surface using a syringe and needle. The syringe's needle is held as close to the surface as possible and in the center of the spinning sample. The plunger is pushed down in a couple of seconds, with the goal of the DEE stream not being so hard that it 'blasts' the perovskite layer away but also not so slow that it drips. After this anti-solvent step, the sample is taken from the spin coater and put onto a hotplate to anneal for 20 minutes at 150 °C.

If a little MABr (or MACL) is added this makes a large difference in the crystallization properties of the thin films. Without it, the films would not turn dark-brown/black when put on the hot plate for annealing but stay yellow and become a bit darker yellow over time. With MABr or MACl, the thin films would turn from light yellow to brown within a second. It was found that you need more MACl than MABr to obtain a similar effect in crystallization.

2.8. Time-resolved photoluminescence

Time-correlated single photon counting measurements of the perovskite thin films on quartz were done on an in-house built setup, PicoQuant PDL 828 "Sepia II" and a PicoQuant HydraHarp 400 multichannel picosecond event timer and TCSPC module. A laser (PicoQuant LDH-D-C-485) with a wavelength of 485 nm was used for excitation with a repetition rate of 0.1 MHz. The emission was measured with a single photon avalanche diode (SPAD) detector (Micro Photon Devices, MPD-5CTD), and to remove the laser light, a long-pass filter (Thorlabs FEL-488) was used. The laser power at 100% was around 15 mW. Also, an ND4 filter was used to decrease the intensity. This setup was used as it was possible to record up to 10 μs, which was necessary for the long lifetimes on quartz substrates.

The photoluminescence (PL) lifetime of perovskite layers has been determined by fitting the TR-PL data to a mono-exponential, bi-exponential, or stretched-exponential model [14]. The model used to fit the data depends on the measured sample, energy levels and electron transfer process in a 'standard' perovskite solar cell [15].

A bi-exponential model is often used when measuring samples containing an HTL or an ETL [16]. In case no charge extraction layers are present on the sample, a stretched exponential was chosen to fit the data to the function $\boldsymbol{f(t) = y_0 + A\, e^{(-t/\tau)^{\beta}}}$, where A is the amplitude, τ is the lifetime, and β is the stretch factor ($0 < \beta < 1$). The stretch factor signifies the heterogeneity of the system. If β is equal

 doi:10.20944/preprints202311.0730.v1

to 1 the function converts to a mono-exponential function. All photophysical data reported here has an estimated error of 5 to 10%.

2.9. XRD measurements of thin films

XRD measurements were performed on thin films on quartz. These were the same samples that were used in the time-resolved photoluminescence measurements. The measurements were performed using a Bruker D2 phase diffractometer operated at 30 kV and 10 mA using a Cu source. The substrates were scanned between $2\theta = 5°$ and $2\theta = 60°$ with a step size of 0.202°. Data analysis was done using Python and Excel.

2.10. Software used

For the analysis of the data, fitting, and plotting of the data, Python programming language was used (version 3.10.8) [17]. For fitting the TCSPC data, the curve fit function from the SciPy library was used. The raw and modified data and the Python code used to make the figures can be found in the accompanying Supporting Information

3. Results and Discussion

3.1. X-ray diffraction

X-ray diffraction (XRD) measurements were performed on thin-layer samples on quartz substrates to get a better insight into the composition of the perovskite thin films. These samples were prepared from precursor solutions with zinc formate and zinc iodide. In Figure 1 and 2, the results can be seen. The observed peaks can also be viewed in Table 3. The perovskites are in an oriented cubic structure as these are in accordance with the diffractions at 13.9° and 28.1°. In the most doped sample (red) some δ-phase can be observed at 11.58°.28 The signal at ~24° is also an indication of the perovskite α-phase but indicates some disorder in the crystal packing of the perovskite. Muscarella et al. observed similar peaks, but could decrease their intensity by aligning the crystals using 3-chloropropylammonium chloride as an additive [18]. It can be observed that the layers that contain more doping have a much higher peak at 12.6°. According to literature, this peak corresponds to PbI2 [18–20]. Such effects have been observed before at high doping [18].

 doi:10.20944/preprints202311.0730.v1

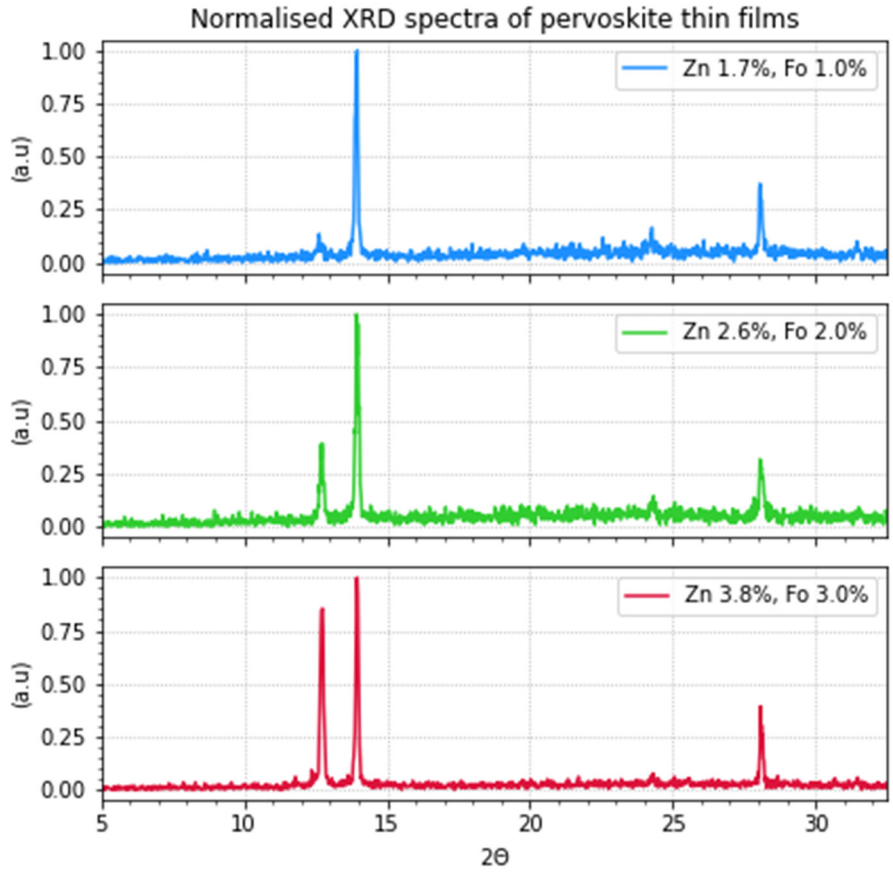

Figure 1. XRD measurements of perovskite thin films on quartz with varying concentrations of zinc and formate, as indicated. The diffraction peaks of the cubic α-phase at 13.9° and 28.1° are clearly visible. The larger diffraction on the left at 12.6° corresponds to the presence of PbI_2. A trace of the perovskite δ-phase can be observed in the highly doped sample at 11.58°.

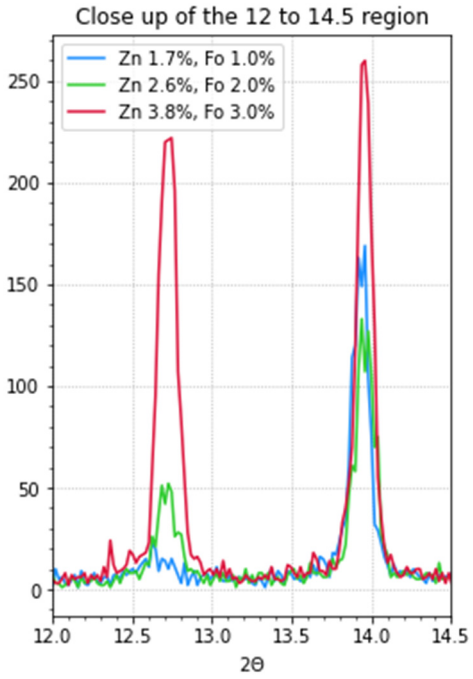

Figure 2. XRD measurements of perovskite thin films on quarts with varying concentrations of zinc and formate. The larger diffraction at on the left at 12.6° corresponds to the presence of PbI_2. (Zoomed in from Figure 1).

 doi:10.20944/preprints202311.0730.v1

Table 3. The results corresponding to the XRD measurements of the three samples. The corresponding graphs can be seen in Figures 1–3. The peak angles are where the peaks are found, the percentage is the normalized height of the spectra, all spectra are normalized relative to the highest peak. The peak value is the not normalized value as measured. The FWHM is the full width at half maximum of the peaks, for the very small peaks it was not possible to calculate this.

Sample code	*Peak (°)*	*%*	*Peak value*	*FWHM (°)*	*designation*
1	*12.6*	*13.6*	*23*	-	*PbI_2*
	13.9	*100%*	*169*	*0.1263*	*α-phase*
	24.3	*16.6%*	*28*	-	
	28.1	*37%*	*63*	*0.1273*	*α-phase*
2	*12.6*	*39%*	*52*	*0.1415*	*PbI_2*
	13.94	*100%*	*133*	*0.1425*	*α-phase*
	24.3	*14%*	*19*	-	
	28.1	*31.5%*	*42*	*0.1727*	*α-phase*
3	*11.58*	*6.2%*	*16*	-	*δ-phase*
	12.6	*85%*	*221*	*0.153*	*PbI_2*
	13.96	*100%*	*260*	*0.118*	*α-phase*
	~24	*7.7%*	*20*	-	-
	28.1	*39%*	*102*	*0.0809*	*α-phase*

3.2. Time-resolved photoluminescence

Time-resolved photoluminescence spectroscopic techniques (TR-PL) have been widely used to study charge separation and extraction in perovskites [14,21–23]. Two advantages of using TR-PL are that it can be done without making contact with the material and that it can be performed with and without attaching a HTL and ETL to the material. [14] In general it can be said that perovskites with longer emission lifetimes can in principle have a greater performance [21,23].

In Figure 3, the results of the TR-PL measurements of three samples can be seen. The details of the fits are combined in Table 4. For each sample, optimal areas of the sample were measured. The dots represent the measurement data, and the lines represent the fits. When comparing the lifetime of the three different samples, 3.7 μs, 0.6 μs, and 1.4 μs for the light, medium, and heavily doped samples respectively, it can be noted that there is no linear correlation to the doping level. However, clearly low zinc doping and low formate doping positively affect the emission lifetime of these samples, to levels that have not been reached so far with single component doping.

 doi:10.20944/preprints202311.0730.v1

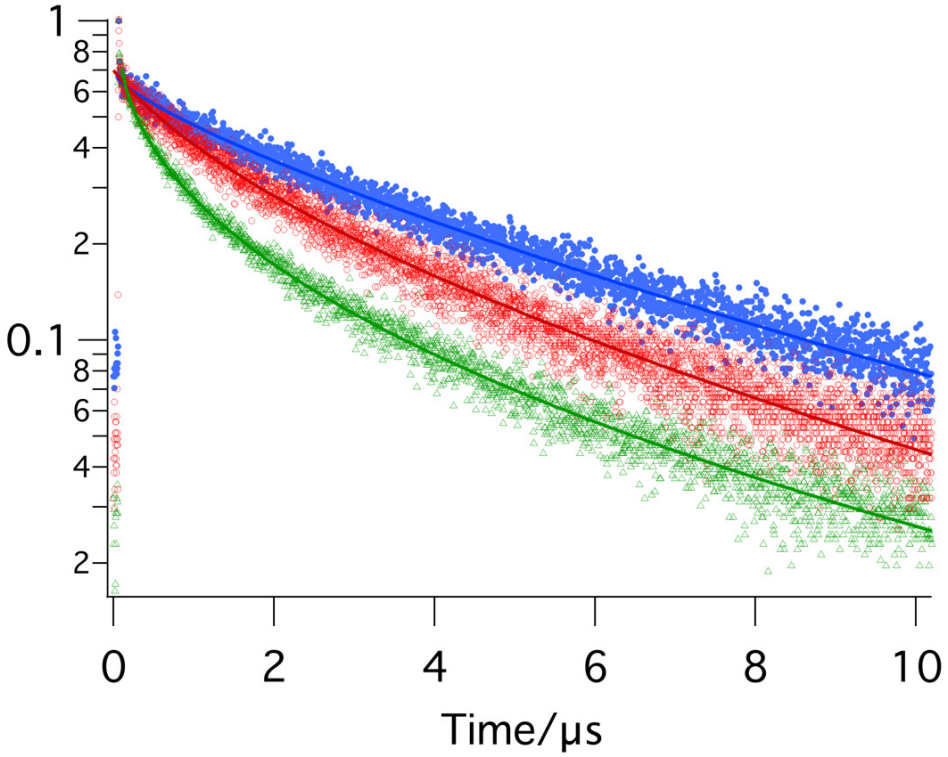

Figure 3. Photoluminescence decays (with stretched exponential fit) of differently doped perovskite thin films. In blue, optimal doping with 1.7% Zn and 1% Fo. In red, non-optimal doping with 3.8% Zn and 3% Fo. In green, non-optimal doping with 2.6% Zn and 2% Fo.

Table 4. The results of the fitting of the TR-PL data with a stretched exponential.

Sample Code	τ (ns)	β	% Zn	% Fo	% total
1	3700	0.77	1.7	1.0	2.7
2	610	0.46	2.6	2.0	4.6
3	1420	0.58	3.8	3.0	6.8

3.2. Thermal stability of doped perovskites

Considering the fact that the pure black α-phase of $FAPbI_3$ perovskite converts to the yellow δ-phase within 24 hours, or a few days, a simple straightforward approach to stability is visual color observation. Figure 4 and 5 show examples of typical observations that can be made. Clearly, samples with 0, 0.5 and 1% $ZnFo_2$ doping have become yellow (or yellow-brown) over the course of 2 weeks, 7 weeks or 6 months. However, doping with higher levels of $ZnFo_2$ (1.3, 2, 3, 4%) results in the observation of black powders (Figures 4 and 5) even after half a year. To determine the deterioration of perovskite samples doped with various amounts of zinc formate, first, visual observation was used. The samples were made by drop-casting solutions with varying concentrations of zinc formate added to the $FAPbI_3$ precursor solution (see experimental section). The powdered samples are shown in plastic cuvettes (Figure 4) or in regular sample vials (Figure 5). These simple visual observations are corroborated by XRD measurement of the thin film that shows the longest emission lifetime. Figure 6 displays that the XRD pattern of an aged spin-coated film shows the same results as the visual observations (see also Table 5, for XRD data). The doped perovskite α-phase of $FAPbI_3$ is thermally stable after six months (black trace) of storage under ambient conditions in a desiccator with regular indoor artificial light. (humidity free, no sunlight).

 doi:10.20944/preprints202311.0730.v1

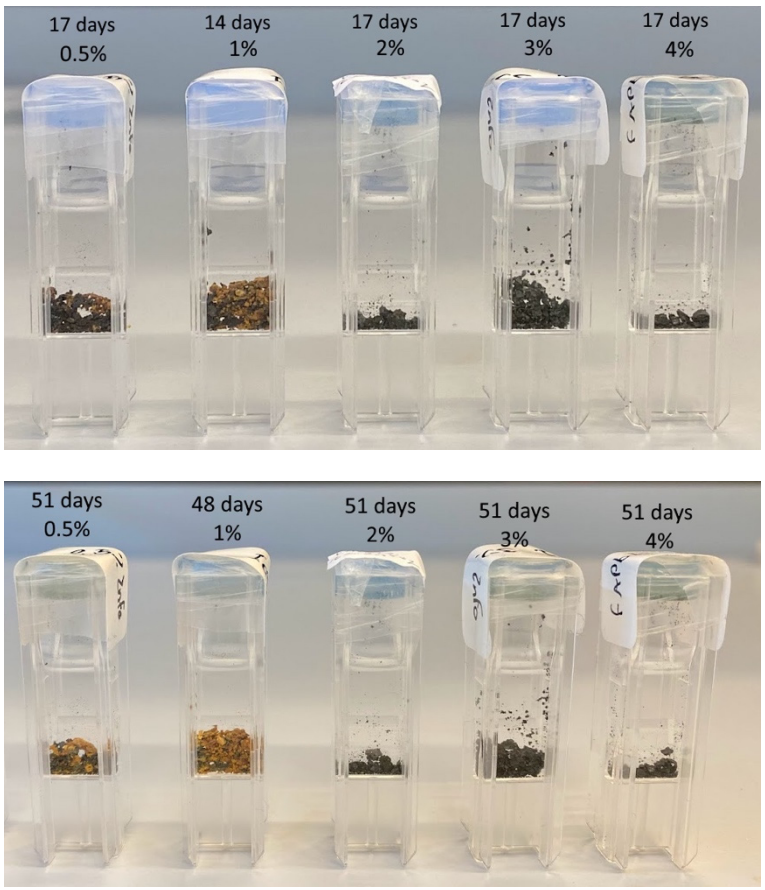

Figure 4. Visual of the discoloration of the black perovskite samples as a function of time. It can be clearly observed that 2% $ZnFo_2$, or more, induces thermal stabilization of the black α-phase.

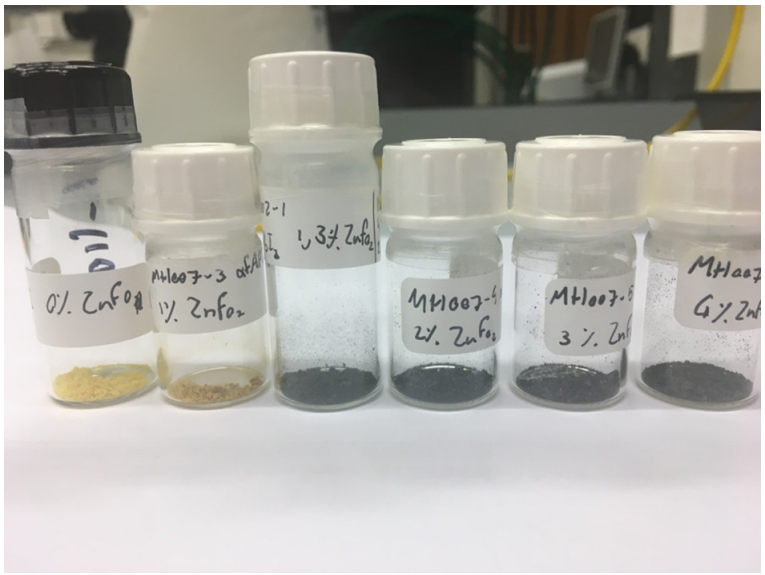

Figure 5. Visual of the discoloration of the black perovskite samples after 6 months. It can be clearly observed that 1.3% $ZnFo_2$ doping, or more, induces thermal stabilization of the α-phase. Samples with 0 or 1% doping are yellow after 6 months. Samples with 1.3, 2, 3, 4% $ZnFo_2$ doping remain black. The sample with 1.3% doping was made for extra precision in determining the limit.

 doi:10.20944/preprints202311.0730.v1

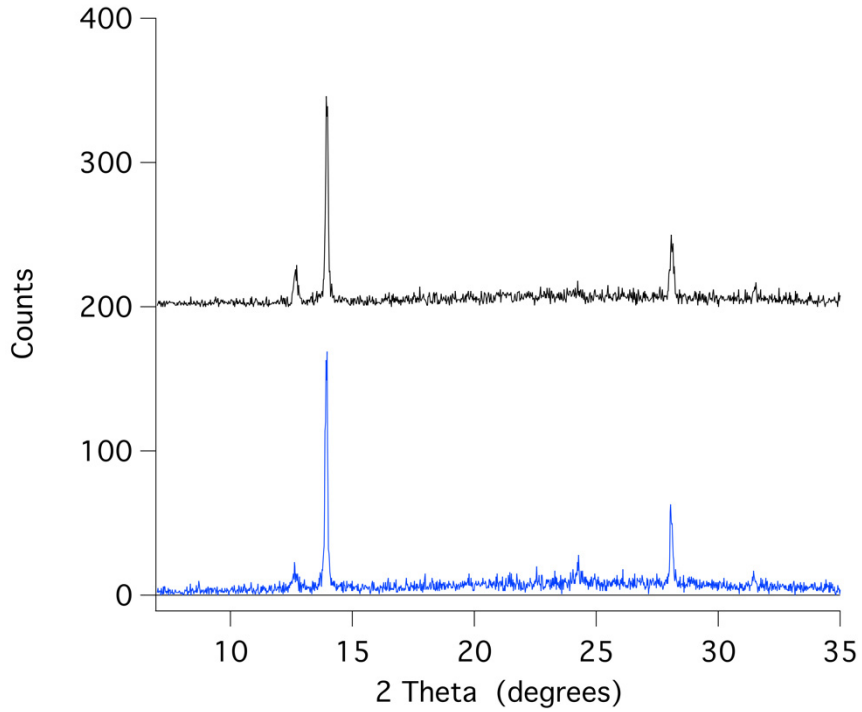

Figure 6. The XRD of spin-coated $FAPbI_3$ thin films optimally doped with zinc (1.7%) and formate (1%) direct after preparation (blue) and six months later (black). The XRD pattern proofs that the black α-phase is thermally stable.

Table 5. The results corresponding to the XRD measurements of the sample of Figure 6, doped with zinc (1.7%) and formate (1%). The peak angles are where the peaks are found, the percentage is the normalized height of the spectra, all spectra are normalized relative to the highest peak. The peak value is the not normalized value as measured. The FWHM is the full width at half maximum of the peaks, for the very small peaks it was not possible to calculate this.

Sample code	*Peak (°)*	*%*	*Peak value*	*FWHM (°)*	*designation*
1	*12.6*	*13.6*	*23*	-	*PbI_2*
	13.9	*100%*	*169*	*0.1263*	*α-phase*
	24.3	*16.6%*	*28*	-	
	28.1	*37%*	*63*	*0.1273*	*α-phase*
1 (aged)	*12.6*	*20%*	*29*	*0.1783*	*PbI_2*
	13.9	*100%*	*146*	*0.1356*	*α-phase*
	24.3	*12%*	*18*	-	
	28.1	*34%*	*50*	*0.1941*	*α-phase*

4. Conclusions and Future Outlook

Zinc formate and zinc iodide doping of perovskite precursor solutions influences the thermal stability and the PL lifetime of $FAPbI_3$ perovskites in a positive way. TR-PL measurements show that the low doping samples have the longest lifetimes. Samples doped with 1.7% zinc and 1% formate show the longest emission lifetimes. The longest lifetime measured in this study was 3.7 µs, using a stretched exponential fit.

Increasing the dopant concentration led to the presence of PbI_2 in the films. To be able to tune the ratio of zinc and formate added to the precursor solution, $Zn(CHOO)_2$ and ZnI_2 are added. Zinc iodide is added to be able to make other ratios than just 1:2 = zinc:formate. In the XRD measurements (Figures 1–3) the increase in PbI_2 is identifiable with an increase in the dopant concentration of the

 doi:10.20944/preprints202311.0730.v1

precursor solution. That the presence of PbI_2 is detrimental to the performance is not a new result, as it is known to be one of the degradation products [20].

Comparing lifetimes obtained from literature can be challenging due to the varying models, measuring devices, parameters used, and sample composition, which may include perovskite layers or other layers. However, three important works to consider are those by Muscarella et al., Jeong et al. and Chen et al., the first two because they were inspirational for this work, and the latter because it has one of the highest lifetimes found in literature [5,28,24]. Muscarella et al. found with glass substrates, a stretched exponential fit with a lifetime of 0.588 μs for a mixed (FA0.85MA0.15)Pb(I2.85Br0.15). This is a typical lifetime for undoped FAPbI3 based thin film materials. When zinc was added, this increased to 0.634 μs, samples of which the crystal structure was aligned using 3-CPACl had an emission lifetime of 1.547 μs. In the paper by Jeong et al., a specific lifetime is not provided, but in previous work by the same group on Cs0.05FA0.85MA0.10Pb(I0.97Br0.03)3 perovskites with a passivation layer of 4-tert-butyl-benzylammonium iodide an emission lifetime of 2.6 μs was reported [25]. Chen et al. found a lifetime of 16 μs, which is the longest lifetime reported. This lifetime was measured in a (FAPbI3)0.9(MAPbBr3)0.05(CsPbBr3)0.05 single crystal perovskite. However, single crystals are not directly comparable to thin films. They are hard to compare because recombination at the perovskite edge usually occurs much faster [14]. The longest lifetime of 3.7 μs reported in this work is long compared to the thin film measurements, indicating that a cell with a small amount of zinc and formate doping can, in principle, perform very well. Furthermore, it was found that without the addition of MABr or MACl, it was impossible to create good perovskite thin films with spin-coating.

The effect of zinc and formate on the stability of the perovskite powders and thin films was investigated. For the powders, it was found that between 1.3% and 4% $ZnFo_2$ doping is where the stability is affected. In the thin films with low doping, no phase change was observed, XRD after 6 months was virtually identical.

Overall, it was found that zinc and formate positively affect the thermal stability of the perovskite α-phase and PL lifetime of $FAPbI_3$. In the grand scheme of events we note that optimal individual doping contents for perovskites (e.g. 2.5% Zn(II) and 2% Fo) do not correspond to optimal contents for synergistic doping agents (1.7% Zn and 1% Fo). Our work indicates that the sum of added doping components should be ~3% (or less). Fine-tuning the ratio of Zn(II) to Fo within this 0-3% doping window may still lead to further improvements of the material properties of perovskites for single junction or tandem cells [26].

Author Contributions: Conceptualization by R.M.W.; all sample preparation as well as the analysis and visualization of the output data by M.M.H.; XRD and time resolved emission measurements: M.M H.; writing—original draft preparation based on the report of MSc internship of M.M.H. at the Molecular Photonics group at UvA within the MSc program Molecular Sciences at UvA; Final writing, review and editing by R.M.W.; supervision by R.M.W.

Funding: This research received no external funding.

Acknowledgments: We thank Imme Schuringa of AMOLF for her help with XRD and TR-PL. We thank the Universiteit van Amsterdam for structural support.

Supporting Information: Data files and analysis files are given in the supporting information. In relation to Research Data Management, this data is also available at the website of this paper posted on Preprints.org.

List of abbreviations

DEE	diethyl ether
PL	photoluminescence
PTFE	polytetrafluoroethylene
DMF	dimethylformamide
DMSO	dimethylsulfoxide
GBL	gamma butyrolactone
τ	lifetime of an excited state

 doi:10.20944/preprints202311.0730.v1

MABr	methylammonium bromide
MACl	methylammonium chloride
TR-PL	Time resolved photoluminescence
Fo	formate anion $(HCO_2)^-$
$FAPbI_3$	Formamidinium lead tri-iodide
XRD	X-ray diffraction

References

1. IPCC, 2021: *Climate Change 2021: The Physical Science Basis. Contribution of Working Group I to the Sixth Assessment Report of the Intergovernmental Panel on Climate Change*[Masson-Delmotte, V., P. Zhai, A. Pirani, S.L. Connors, C. Péan, S. Berger, N. Caud, Y. Chen, L. Goldfarb, M.I. Gomis, M. Huang, K. Leitzell, E. Lonnoy, J.B.R. Matthews, T.K. Maycock, T. Waterfield, O. Yelekçi, R. Yu, and B. Zhou (eds.)]. Cambridge University Press, Cambridge, United Kingdom and New York, NY, USA, https://dx.doi.org/10.1017/9781009157896 (accessed 2023-04-13)
2. Ritchie, H.; Roser, M.; Rosado, P. (2022) - "Energy". Published online at OurWorldInData.org. Retrieved from: https://ourworldindata.org/energy (accessed 2023-04-13)
3. Kojima, A.; Teshima, K.; Shirai, Y.; Miyasaka, T. Organometal Halide Perovskites as Visible-Light Sensitizers for Photovoltaic Cells. *Journal of the American Chemical Society* **2009**, *131* (17), 6050–6051. https://doi.org/10.1021/ja809598r.
4. NREL. *Best Research-Cell Efficiency Chart*. https://www.nrel.gov/pv/cell-efficiency.html (accessed 2023-04-13)
5. Muscarella, L. A.; Petrova, D.; Jorge Cervasio, R.; Farawar, A.; Lugier, O.; McLure, C.; Slaman, M. J.; Wang, J.; Ehrler, B.; von Hauff, E.; Williams, R. M. Air-Stable and Oriented Mixed Lead Halide Perovskite (FA/MA) by the One-Step Deposition Method Using Zinc Iodide and an Alkylammonium Additive. *ACS Appl. Mater. Interfaces* **2019**, *11* (19), 17555–17562. https://doi.org/10.1021/acsami.9b03810.
6. Kooijman, A.; Muscarella, L.A.; Williams, R.M. Perovskite Thin Film Materials Stabilized and Enhanced by Zinc(II) Doping. *Appl. Sci.* **2019**, *9*, 1678. https://doi.org/10.3390/app9081678
7. Ye, S., Rao, H., Feng, M., Xi, L., Yen, Z., Seng, D. H. L., Xu, Q., Boothroyd, C., Chen, B., Guo, Y., Wang, B., Salim, T., Zhang, Q., He, H., Wang, Y., Xiao, X., Lam, Y. M., & Sum, T. C. Expanding the low-dimensional interface engineering toolbox for efficient perovskite solar cells. *Nature Energy*. **2023**, 8, 284–293. https://doi.org/10.1038/s41560-023-01204-z
8. Jeong, J.; Kim, M.; Seo, J.; Lu, H.; Ahlawat, P.; Mishra, A.; Yang, Y.; Hope, M. A.; Eickemeyer, F. T.; Kim, M.; Yoon, Y. J.; Choi, I. W.; Darwich, B. P.; Choi, S. J.; Jo, Y.; Lee, J. H.; Walker, B.; Zakeeruddin, S. M.; Emsley, L.; Rothlisberger, U.; Hagfeldt, A.; Kim, D. S.; Grätzel, M.; Kim, J. Y. Pseudo-Halide Anion Engineering for α-FAPbI3 Perovskite Solar Cells. *Nature* **2021**, *592* (7854), 381–385. https://doi.org/10.1038/s41586-021-03406-5.
9. Tong, G.; Son, D.-Y.; Ono, L. K.; Kang, H.-B.; He, S.; Qiu, L.; Zhang, H.; Liu, Y.; Hieulle, J.; Qi, Y. Removal of Residual Compositions by Powder Engineering for High Efficiency Formamidinium-Based Perovskite Solar Cells with Operation Lifetime over 2000 h. *Nano Energy* **2021**, *87*, 106152. https://doi.org/10.1016/j.nanoen.2021.106152
10. Tang, G.; You, P.; Tai, Q.; Wu, R.; Yan, F. Performance Enhancement of Perovskite Solar Cells Induced by Lead Acetate as an Additive. **2018**, 9. https://doi.org/10.1002/solr.201800066.
11. Zhao, J.; O. Fürer, S.; P. McMeekin, D.; Lin, Q.; Lv, P.; Ma, J.; Liang Tan, W.; Wang, C.; Tan, B.; R. Chesman, A. S.; Yin, H.; D. Scully, A.; R. McNeill, C.; Mao, W.; Lu, J.; Cheng, Y.-B.; Bach, U. Efficient and Stable Formamidinium–Caesium Perovskite Solar Cells and Modules from Lead Acetate-Based Precursors. *Energy & Environmental Science* **2023**, *16* (1), 138–147. https://doi.org/10.1039/D2EE01634F.
12. Li, M.; Li, H.; Zhuang, Q.; He, D.; Liu, B.; Chen, C.; Zhang, B.; Pauporté, T.; Zang, Z.; Chen, J. Stabilizing Perovskite Precursor by Synergy of Functional Groups for NiOx-Based Inverted Solar Cells with 23.5 % Efficiency. *Angewandte Chemie International Edition* **2022**, *61* (35), e202206914. https://doi.org/10.1002/anie.202206914.
13. Griffin, J.; Hassan, H.; Spooner, E. *Spin Coating: Complete Guide to Theory and Techniques*. Ossila. https://www.ossila.com/en-eu/pages/spin-coating (accessed 2022-09-15).
14. Baloch, A. A. B.; Alharbi, F. H.; Grancini, G.; Hossain, M. I.; Nazeeruddin, Md. K.; Tabet, N. Analysis of Photocarrier Dynamics at Interfaces in Perovskite Solar Cells by Time-Resolved Photoluminescence. *J. Phys. Chem. C* **2018**, *122* (47), 26805–26815. https://doi.org/10.1021/acs.jpcc.8b07069.
15. Marchioro, A.; Teuscher, J.; Friedrich, D.; Kunst, M.; van de Krol, R.; Moehl, T.; Grätzel, M.; Moser, J.-E. Unravelling the Mechanism of Photoinduced Charge Transfer Processes in Lead Iodide Perovskite Solar Cells. *Nature Photonics* **2014**, *8*, 250–255. https://doi.org/10.1038/nphoton.2013.374
16. Stranks, S. D.; Eperon, G. E.; Grancini, G.; Menelaou, C.; Alcocer, M. J. P.; Leijtens, T.; Herz, L. M.; Petrozza, A.; Snaith, H. J. Electron-Hole Diffusion Lengths Exceeding 1 Micrometer in an Organometal Trihalide Perovskite Absorber. *Science* **2013**, *342* (6156), 341–344. https://doi.org/10.1126/science.1243982.

17. *Welcome to Python.org*., https://www.python.org/ (accessed 2022-11-25).
18. Muscarella, L. A.; Petrova, D.; Cervasio, R. J.; Farawar, A.; Lugier, O.; McLure, C.; Slaman, M. J.; Wang, J.; Hauff, E. von; Williams, R. M. Enhanced Grain-Boundary Emission Lifetime and Additive Induced Crystal Orientation in One-Step Spin-Coated Mixed Cationic (FA/MA) Lead Perovskite Thin Films Stabilized by Zinc Iodide Doping. **2017**. https://doi.org/10.26434/chemrxiv.5484073.v2.
19. Nie, W.; Tsai, H.; Asadpour, R.; Blancon, J.-C.; Neukirch, A. J.; Gupta, G.; Crochet, J. J.; Chhowalla, M.; Tretiak, S.; Alam, M. A.; Wang, H.-L.; Mohite, A. D. High-Efficiency Solution-Processed Perovskite Solar Cells with Millimeter-Scale Grains. *Science* **2015**, *347* (6221), 522–525. https://doi.org/10.1126/science.aaa0472.
20. Huang, J.; Tan, S.; Lund, P. D.; Zhou, H. Impact of H2O on Organic-Inorganic Hybrid Perovskite Solar Cells. *Energy and Environmental Science* **2017**, *10* (11), 2284–2311. https://doi.org/10.1039/c7ee01674c.
21. Bi, D.; El-Zohry, A. M.; Hagfeldt, A.; Boschloo, G. Unraveling the Effect of PbI2 Concentration on Charge Recombination Kinetics in Perovskite Solar Cells. *ACS Photonics* **2015**, *2* (5), 589–594. https://doi.org/10.1021/ph500255t.
22. Handa, T.; Tex, D. M.; Shimazaki, A.; Wakamiya, A.; Kanemitsu, Y. Charge Injection Mechanism at Heterointerfaces in CH3NH3PbI3 Perovskite Solar Cells Revealed by Simultaneous Time-Resolved Photoluminescence and Photocurrent Measurements. *J. Phys. Chem. Lett.* **2017**, *8* (5), 954–960. https://doi.org/10.1021/acs.jpclett.6b02847.
23. Fang, H.-H.; Wang, F.; Adjokatse, S.; Zhao, N.; Even, J.; Loi, M. A. Photoexcitation Dynamics in Solution-Processed Formamidinium Lead Iodide Perovskite Thin Films for Solar Cell Applications. *Light Sci Appl* **2016**, *5* (4), e16056–e16056. https://doi.org/10.1038/lsa.2016.56.
24. Chen, L.; Tan, Y.-Y.; Chen, Z.-X.; Wang, T.; Hu, S.; Nan, Z.-A.; Xie, L.-Q.; Hui, Y.; Huang, J.-X.; Zhan, C.; Wang, S.-H.; Zhou, J.-Z.; Yan, J.-W.; Mao, B.-W.; Tian, Z.-Q. Toward Long-Term Stability: Single-Crystal Alloys of Cesium-Containing Mixed Cation and Mixed Halide Perovskite. *J. Am. Chem. Soc.* **2019**, *141* (4), 1665–1671. https://doi.org/10.1021/jacs.8b11610.
25. Zhu, H.; Liu, Y.; Eickemeyer, F. T.; Pan, L.; Ren, D.; Ruiz-Preciado, M. A.; Carlsen, B.; Yang, B.; Dong, X.; Wang, Z.; Liu, H.; Wang, S.; Zakeeruddin, S. M.; Hagfeldt, A.; Dar, M. I.; Li, X.; Grätzel, M. Tailored Amphiphilic Molecular Mitigators for Stable Perovskite Solar Cells with 23.5% Efficiency. *Advanced Materials* **2020**, *32* (12), 1907757. https://doi.org/10.1002/adma.201907757.
26. Marchant, C.; Williams, R. M. Perovskite / Silicon Tandem Solar Cells – Compositions for Improved Stability and Power Conversion Efficiency. (Accepted) *Photochem. Photobiol. Sci.* **2023**. https://doi.org/10.1007/s43630-023-00500-7